Empirical Modeling of Pneumatic Artificial Muscle

K. C. Wickramatunge and T. Leephakpreeda

Abstract— **Pneumatic Artificial Muscle (PAM) yields natural muscle-like actuator with high force to weight ratio, soft and flexible structure, and adaptable compliance for rehabilitation and prosthetic appliances to the disabled. To obtain optimum design and usage, there is significance to understand mechanical behavior of the PAM. In this study, experimental results reveal empirical modeling for relations of physical variables in contraction and air-pressure of the PAM to mechanical characteristics, that is stiffness and force of the PAM available in market.**

Index Terms— **Empirical modeling, mechanical spring system, pneumatic artificial muscle, stiffness parameter.**

I. Introduction

A Pneumatic Artificial Muscle (PAM) is a pneumatic actuator for converting pneumatic power to pulling force. The PAM yields advantage characteristics over conventional pneumatic cylinders such as high force to weight ratio, flexible movements, variable installation possibilities, no mechanical wear, minimal compressed-air consumption, size availability, low cost and extreme safe for human use. However, this PAM exhibits highly non-linear characteristics due to compressibility of air, inherent properties of elastic-viscous material. This makes the PAM difficult to modeling and controlling. Currently, existing models do not describe every stage of the mechanical behavior well; therefore, further improved model is still required.

The PAM was first invented in 1950s by the physician, Joseph L. McKibben and it was used for artificial limb for handicapped hands [1]. In 1980s, redesigned and more powerful PAM was introduced by Bridgestone Company and it was used for painting applications, some applications to assist disabled individuals and service robotics. Up to now, the PAM has been used for different kind of humanoid applications and advanced robotic applications. The PAM is mainly used as robotic actuators in applications where compliance and low power to weight ratio are important, e.g. walking/running machines or even humanoid robots [2]. Nowadays, Shadow Group of Company and FESTO are producing different kind of PAM for robotic and industrial applications.

K. C. Wickramatunge is with Sirindhorn International Institute of Technology, Thammasat University - Rangsit Campus, P.O.Box 22, Pathum Thani 12121, Thailand. (phone: +66 (0) 2986 9009, 2986 9101; fax: +66(0) 2986 9112-3; e-mail: kanchanawi@siit.tu.ac.th).

T. Leephakpreeda is with Sirindhorn International Institute of Technology, Thammasat University - Rangsit Campus, P.O.Box 22, Pathum Thani 12121, Thailand. (e-mail: thanan@siit.tu.ac.th).

Typically, the PAM has been made of thin rubber tube (bladder) covered by a braided mesh shell and two ends were closed, one being air inlet and other connected with the load. When the PAM connects with the pressurized air supply, the internal bladder tends to increase its volume against the braided mesh shell but non–extensibility of the braided mesh threads cause to shorten the actuator and produce pulling forces if it is connected with the load. The new type of the PAM has been introduced by FESTO recently. Its basic concept involves the wrapping of a watertight, flexible hose with non-elastic fibers arranged in a rhomboidal fashion. This results in a three-dimensional grid pattern, and when compressed air is introduced into the PAM, the grid pattern is deformed. A pulling force is generated in the axial direction, resulting in a shortening of the muscle as air pressure is increased.

Different models were proposed to describe the behavior of the PAM. Among these models, Chou and Hannaford model [3] and Tondu and Lopez model [1] are widely used. These models are based on the hypothesis on virtual works of an infinitely thin inner tube and continuously cylindrical shape. For example, these models still have limitations of predictions on behavior of the PAM in no-load conditions.

Furthermore, pulling force, length, air pressure, diameter and material properties are the major parameters of the PAM on dynamical behaviors and the relationships between these parameters are greatly changed form one PAM to another PAM. In [4], physical configuration and the behavior of the PAM hinted the variable stiffness similar to spring-like characteristics. In this study, the PAM system will be regarded as a mechanical spring system. An empirical method for modeling the PAM will be proposed and discussed with both theoretical and experimental approach. Finally, experimental results will be compared with the results of the empirical model.

II. Experimental Setup

A diagram of the experimental setup illustrated in Fig.1 is capable of provide real-time collecting data of the PAM length, the air pressure within PAM and the pulling force during tension. The pulling forces were generated by a hydraulic cylinder. The load cell mounted at one fixed end of the PAM was implemented to obtain the pulling forces. The other movable end of the PAM was attached with a linear potentiometer for measurement of the length of the PAM. Pressure transducer connected at the air inlet of the PAM was used to observe the air pressure. As mentioned above, all measurement devices were interfaced to the computer through data acquisition card.

In this experiment, FESTO branded PAM was used with

the nominal diameter of 2 cm and the length of 30 cm. The air pressure within the PAM supplied by an air compressor was ranged between 1.0 bar and 5 bar (gage pressure) while the pulling forces were varied between 0 –1000 N.

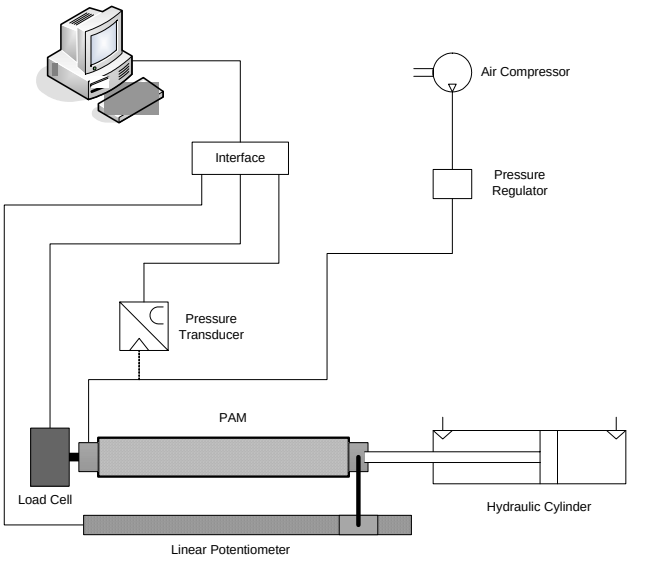

(a)

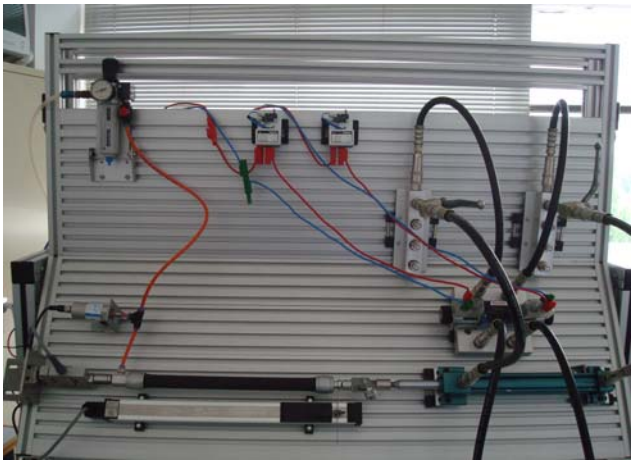

(b)

Figure 1: *Experimental Setup: (a) Diagram and (b) Photograph.*

III. Description of the Parameters

First, the working principles of the PAM described here gives an insight to derive the empirical model. Initially, the PAM keeps its original length at the zero gage pressure or the atmospheric pressure without pulling any load and this length denoted as L_o. When the air pressure P within the PAM changes, e.g. $P_2 > P_1$, the PAM contracts until its come to its new equilibrium length according to that new air pressure within the PAM as shown in Fig.2 (a). In this study, this maximum contraction length dependent upon the air pressure is called unstretched length and it is denoted as L_u. It can be seen that the unstretched length change according to the air pressure as given in the graph of Fig. 2(b). As shown in Fig. 2(c), the contracted PAM tends to increase its length according to the pulling force F, which it is exerted with. The instantaneous length of the muscle is considered L. Therefore, the stretched length, L_s is defined as the length difference between instantaneous length and unstretched length. It should be noted that the PAM has a certain working length within the stretched length for a given pressure.

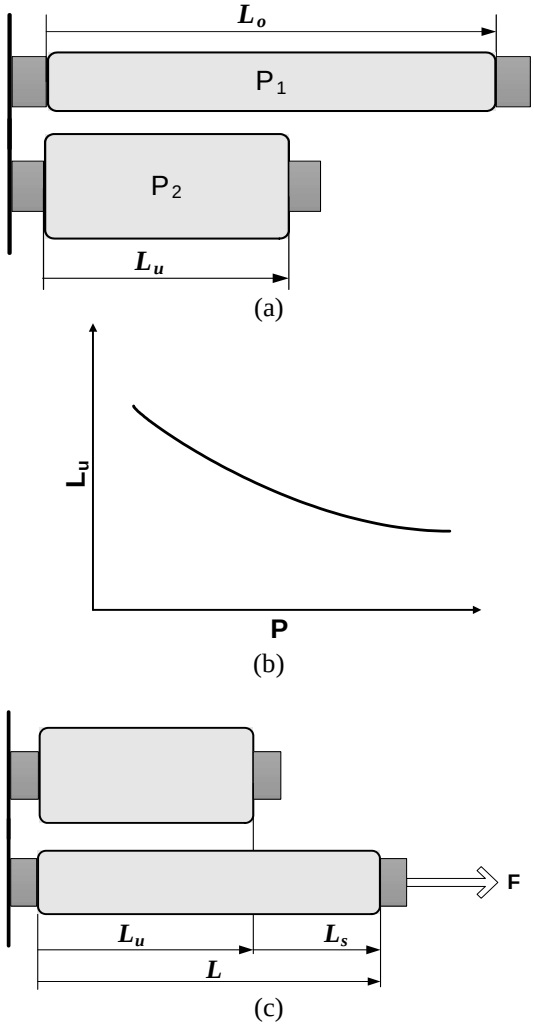

Figure 2: *Illustration of PAM parameters; (a) initial and final length of the PAM at the operating air pressure without pulling force;(b) variation of unstretched length against the air pressure within PAM; (c) length definitions when PAM exerted by pulling force.*

IV. Method of Modeling the PAM

From previous section, it can be concluded that functions of both PAM and mechanical spring system show significantly similar characteristics when it is operated with or without pulling forces in working conditions. The physical functionality of these two systems can be presented as shown in Fig.3. Both the PAM and the spring system show similar behavior when the pulling force is applied. Conventionally, the stiffness of the spring system is constant and it is dependent upon the material properties and the geometry of the spring. On the other hand, the stiffness of the PAM is a variable parameter and it depends upon not only the above mentioned properties but also the operating air pressure within the PAM.

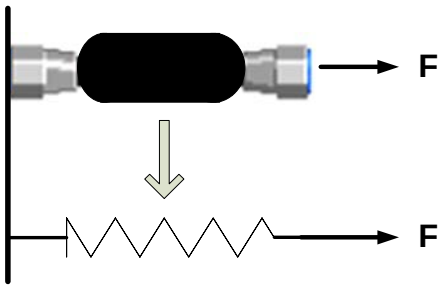

Figure 3: *(a) Equivalent system diagram of Pneumatic muscle and spring system.*

Based on experimental observations later, the pulling forces acting on the muscle can be modeled in the same as the force acting on the mechanical spring system. The stiffness parameter of the muscle denotes as K and it is considered a function of the operating air pressure, P (Gage Pressure) and the stretched length, L_s. The elastic forces adversely generated by the PAM is denoted by $F_{elastic}$ and the expression given in Eq.1 shows the proposed model for the Force acting on the PAM as a function of K and L_s.

$$F_{elastic} = K(P, L_s) L_s \quad (1)$$

V. Results and Discussion

The unstretched length of the PAM (mentioned in section III) was measured by increasing the pressure 0-5 bar (gage pressure) without applying the pulling force. The plots given in Fig. 4 show the behavior of the unstretched length according to the air pressure within the PAM. It can be seen that the unstretched length decreases as the air pressure within the PAM increases as expected. The more the air pressure, the greater the contraction. This result can be used to determine the unstretched length for given air pressure.

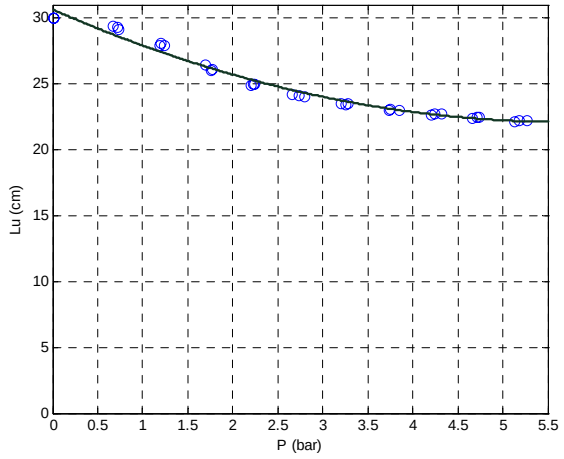

Figure 4: *Plot of unstressed length against air pressure.*

In this section, the mechanical behaviors of the PAM are drawn by using the experimental setup, which has been mentioned in the section II. Initially, the PAM is maintained to be steady at the unstretched position by supplying a constant pressure of the compressed air. After that, the pulling force is applied increasingly by the hydraulic cylinder. The PAM is stretched in such way that the pulling force balances against the elastic force within the working range. The length of the PAM L is recorded until the L reached to L_o. In the same consideration for reverse direction, the L is recorded by reducing the pulling force until the L reached to the L_u again. Fig.5 shows the experimental results of the stretched length in the working range of air pressure in both forward and backward direction.

The stretched lengths increase as shown in Fig. 5 with solid lines with upward heading arrows. On the other hand, the stretched lengths decrease as shown in Fig. 5 with solid lines with downward heading arrows. It can be observed that the hysteresis nonlinearity takes place from effects on increasing or decreasing the pulling force at various air pressures. It should be noted that the stretched length at the low pressure is shorter than that at the high pressure because the unstretched length is longer at low pressures seen in Fig. 4. These results indicate that the stiffness parameters K in Eq. (1) are different for cases of increasing and decreasing the pulling forces.

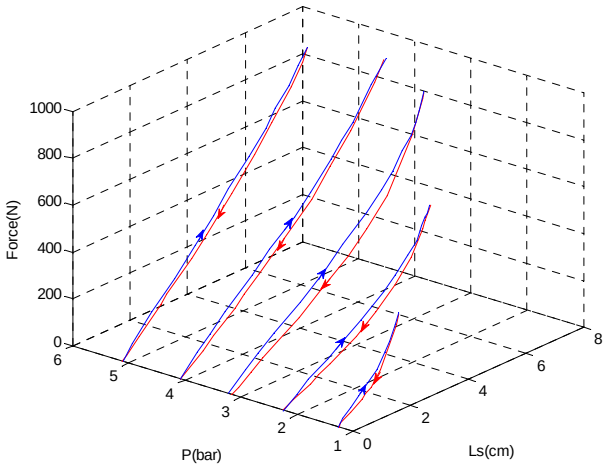

Figure 5: *Experimental results of contraction and extraction of the PM (Length =30cm, diameter =2cm).*

In this study, the stiffness parameter K is taken as a second order polynomial function of L_s and P and it is expressed in Eq.2. However, an universal approximation method with fuzzy logic or neural network can be used as alternative choice for accuracy viewpoint [5].

$$K = a_o P^2 + a_1 P L_s + a_2 L_s^2 + a_3 \quad (2)$$

where a_o, a_1, a_2 *and* a_3 are constant coefficients, which can be obtained from experimental data.

To yield the best fit, the range of the air pressure is divided into the operating conditions where the air-pressure of 0-2.5 bar is considered the low pressure range and the air pressure of 2.5-5.0 bar is considered the high pressure range. In general, the selection of pressure range might be varied according to experimental data. The unknown coefficients of the Eq. 2 are determined by applying the least squared method to the experimental data in Fig. 5. The values of coefficients are obtained and given in the Table 1.

Table 1 *Values of coefficients in K*

Constant	Extraction		Contraction	
	Low pressure range	High pressure range	Low pressure range	High pressure range
a_o	-2.299	4.182	-2.977	3.837
a_1	-5.741	-3.127	-5.890	-2.389
a_2	2.741	1.818	3.203	1.850
a_3	119.304	70.377	104.824	53.021

According to Table 1, the plots of the stiffness parameter, *K* in Eq. 2 for the air pressure of 1-5 bar and stretched length range of 0-7 cm is illustrated in Fig. 6. The cases of extraction and contraction are presented in Fig. 6(a) and Fig. 6(b) respectively. It should be noted that plots in the section A show the results from Eq. 2 within the working length while the section B is out of the stretched length. From observation, the value of the stiffness parameter increases while the stretched length increases for given air pressure. However, for a given stretched length, the value of stiffness parameter decreases as the air pressure increased at low pressure and it increases afterward as the air pressure increases at high pressure. This might be because the behavior of the rubber material itself is dominant at low pressure while the behavior of the PAM is developed at high pressure after all.

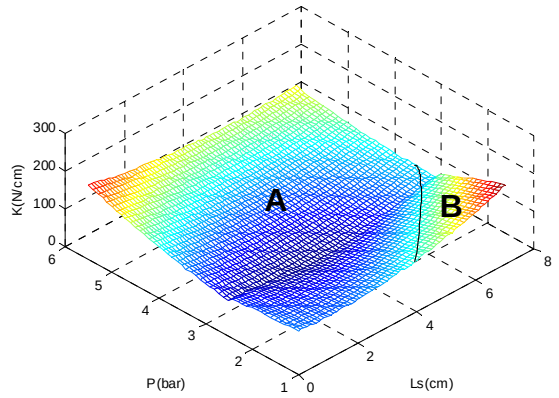

(a)

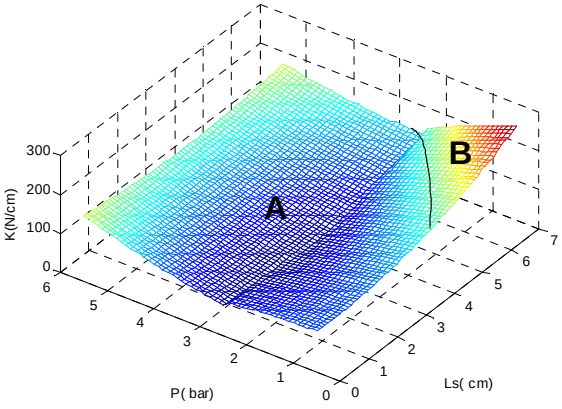

(b)

Figure 6: *Stiffness parameter K: (a) increasing stretched length and (b) decreasing stretched length.*

Fig.7 shows the comparison between the validating data from experiment and results of the empirical model resulted from Eq. (1) in cases of extraction and contraction from changing the pulling forces. It can be seen that the results of the model can be fitted to validating data well.

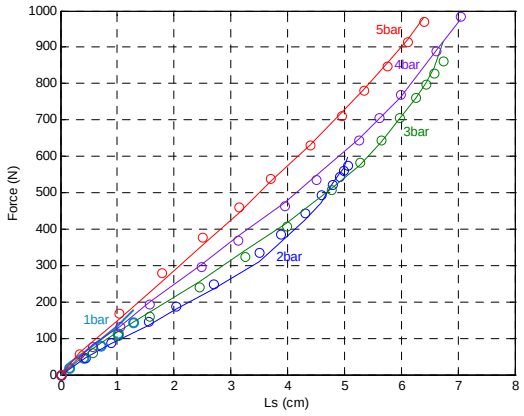

(a)

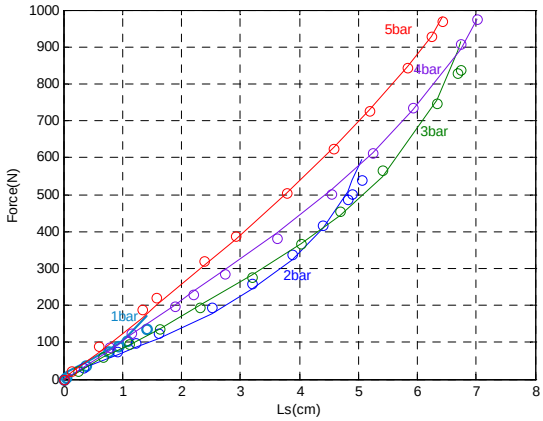

(b)

Figure 7: *Comparison between experimental results (circles) and simulation results (solid lines): (a) extraction and (b) contraction.*

To see the performance of the proposed model, the dynamic behaviors of the PAM are studied. The empirical model is implemented to determine the position/length of the PAM when the pulling force exerts on the PAM in time. In case study, the PAM is initially kept at its unstretched position by the air pressure of 5 bar as depicted in Fig. 8. The PAM is extracted by the hydraulic cylinder. The pulling force is increased from 0 N to 600 N in 1 second. It can be observed that the air pressure increases since the volume of the PAM decreases and in turn the air pressure rises up. The air pressure and the pulling force are inputted to the model in Eq. (1). The simulation results of the length of the PAM can be obtained and compared to the experimental results as shown in the last plot of Fig. 8. The simulation results agree with the experimental results very well.

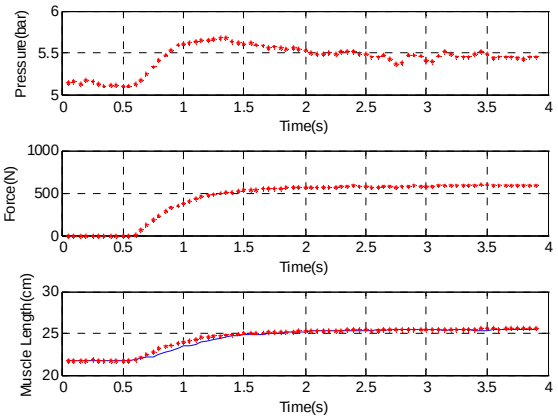

Figure 8: *Comparison between experimental results (dotted line) and simulation results (solid line) during step change of pulling force*

VI. Conclusion

In certain situations, the impotency of the PAM is higher than the conventional pneumatic cylinders such as humanoid applications. The developed empirical model gives a concrete and effective description to understand the mechanical behavior of the PAM for design and usage. The agreement of simulation results on the experimental results confirms the viability of the proposed techniques.

Acknowledgment

Financial support for this research was provided by the Thailand Research Fund: TRF Research scholars-RSA5180011. Authors sincerely thank B. Chompooborisuth and P. Chutikanon for their assistance in experiment.

References

[1] Tondu, B., and P. Lopez," Modeling and control of McKibben artificial muscle robot actuators", *IEEE Control Systems Magazine* Vol. 20, No. 2, 2000, pp. 15-38.

[2] Daerden, F., and D. Lefeber," Pneumatic artificial muscles: Actuators for robotics and automation", *European Journal of Mechanical and Environmental Engineering* Vol. 47, No. 1, 2002, pp. 11-21.

[3] Chou, C.P., and B. Hannaford," Measurement and modeling of McKibben pneumatic artificial muscles", *IEEE Transactions on Robotics and Automation* Vol. 12, No. 1, 1996, pp. 90-102.

[4] Chou, C.-P., and B. Hannaford, "Static and dynamic characteristics of McKibben pneumatic artificial muscles", *Proceedings - IEEE International Conference on Robotics and Automation*, 1994, pp. 281-286.

[5] Leephakpreeda, T.," Novel determination of differential-equation solutions: Universal approximation method", *Journal of Computational and Applied Mathematics* Vol. 146, No. 2, 2002, pp. 443-457.